PHYSICAL REVIEW B VOLUME 8, NUMBER 8 15 OCTOBER 1973

Low-Temperature Heat Transport in Solid HD[†]

J. H. Constable and J. R. Gaines
Department of Physics, Ohio State University, Columbus, Ohio 43210

(Received 7 May 1973)

The thermal conductivity of solid HD has been measured and compared with theory over the temperature range 4–0.2 K. Since the sample remained frozen over the entire period in which the measurements were made, the H_2 and D_2 impurities, as well as the other crystal defects, were assumed fixed in the lattice. However, the concentration of the $J = 1$ orthohydrogen (o-H_2) and paradeuterium impurities in the sample changed through the slow $J = 1$ to $J = 0$ conversion taking place in the solid. The rate of conversion and consequently the $J = 1$ concentration was determined by measuring, as a function of time, the heat of conversion resulting from $J = 1$ to $J = 0$ transitions. Because of the variation in the $J = 1$ concentration, it was possible to separate the thermal resistivity into a ($J = 1$)-dependent part and a part independent of $J = 1$ concentration. The resistivity resulting from phonon scattering by $J = 1$ molecules was compared to existing theory for two-phonon Raman scattering by o-H_2 molecules in a parahydrogen solid. At the lowest temperatures, the temperature dependence of this resistivity was too large to be accounted for by a two-phonon process. It is suggested that a one-phonon process is responsible for the increase in the resistivity at low temperatures. The results of a calculation are given to demonstrate the plausibility of this argument. Below 1 K, the ($J = 1$)-independent conductivity can be adequately fitted by a T^3 temperature dependence. From this dependence it was inferred that the sample was polycrystalline. Above 1 K, the ($J = 1$)-independent conductivity is dominated by the presence of the H_2 and D_2 isotopic impurities. The techniques used to measure these impurity concentrations are described in detail.

I. INTRODUCTION

The current feasibility of maintaining low temperatures and high magnetic fields simultaneously has stimulated considerable interest in the production of a high static nuclear-spin polarization. A problem of particular practical importance has been the production of a polarized proton target using the solid hydrogens. However, for these samples to be useful as polarized targets, it is necessary to remove a large quantity of heat from the hydrogen sample. It is the object of this paper to analyze the heat-removal process in the nearly pure $J = 0$ solid hydrogens and to present a reasonable explanation for some of the recently unexplained results.

Measurements by Bohn and Mate[1] of the thermal conductivity of solid parahydrogen, p-H_2, containing between 0.2 and 5-mole % orthohydrogen, o-H_2, have shown a marked dependence of the thermal conductivity on the o-H_2 concentration. This dependence has been partially explained by the theory of Ebner and Sung.[2] However, at low temperatures the theory predicts a conductivity which should be proportional to $c^{-2}T^2$ (where c is the o-H_2 concentration and T is the temperature), while the experimental results indicate a conductivity which is proportional to $c^{-1}T^3$.

Due to the T^3 dependence of the low-temperature thermal-conductivity data of Bohn and Mate, some speculation has arisen that this dependence might be due to phonon scattering from crystalline boundaries in a powder whose average dimensions were determined by the concentration of the $J = 1$ impurities present (where J is the rotational quantum number). In order for the HD thermal-conductivity measurements reported here to add any significantly new information, this question must be resolved. This was done by forming only one HD crystal and letting the natural conversion of the impurities from the $J = 1$ state to the $J = 0$ state change the $J = 1$ concentration. Thus during the experiment the crystalline boundaries and mass defects were frozen in while the $J = 1$ concentration was varied. It should be noted that the analogous experiment in H_2 is impossible due to rotation diffusion of the $J = 1$ impurities.[3]

The experimental results on HD reported here should be qualitatively similar to those of p-H_2 since both are $J = 0$ hydrogen solids containing a small number of $J = 1$ impurities. Similarities between the results for p-H_2 and HD were indeed found. The unexpectedly large T^{-3} thermal resistivity found for p-H_2 was observed for HD but was found to be independent of the ortho-para ratio. The c^2T^{-2} dependence of the thermal resistivity on the $J = 1$ concentration predicted by Ebner and Sung was also found. In addition to these resistive mechanisms, the low-temperature data showed another scattering mechanism which has been adequately fitted to a resistivity term proportional to cT^{-7}. The concentration and temperature dependence of this term was arrived at on the basis of a calculation of the resistivity resulting from a first-order phonon scattering by the rotational substates. This calculation is discussed in Sec. II together with the theory of the thermal conductivity in the nearly pure $J=0$ solid hydrogens.

In Sec. III the experimental measurements of the thermal conductivity are presented. Results are given for the H_2 and D_2 impurity concentrations, the $J=1$ to $J=0$ conversion rate, and the resulting $J=1$ concentration as a function of time. In addition, a discussion is given of the heat conducted across the interface between the hydrogen solid and the substance in contact with it. Preliminary measurements of this contact resistance have indicated that it is anomalously high[4,5] in comparison to that predicted from the Khalatnikov theory[6] of boundary resistance. An explanation is given to account for these observations and the ones made in this experiment.

II. THEORY OF THERMAL CONDUCTIVITY IN THE $J=0$ SOLID HYDROGENS

A. Properties of Solid Hydrogen H_2, HD, and D_2

The solid hydrogens are molecular solids which exhibit all the properties of dielectric solids in addition to the unique properties resulting from the rotational degrees of freedom. The Debye temperatures, Θ_D, for H_2 and D_2 have been determined by various investigations to be nearly the same, thus indicating a large anharmonicity in the solids. The Debye temperatures for H_2 [1,7-10] range between 109 and 128 K while those for D_2 [7,8,10] range between 106 and 114 K. Considering these values, we have taken rather arbitrarily the Debye temperature for HD to be $\Theta_D = 112$ K in the following discussion.

Symmetry under interchange of the nuclei in the homonuclear molecules H_2 and D_2 gives rise to the two rotational modifications, ortho and para hydrogen and deuterium. Since HD is a heteronuclear molecule, it has no symmetry requirements under nuclear interchange. The transition rate between the ortho and para states is relatively slow compared to the usual experimental times and thus one can make measurements in samples containing various ortho-para ratios. The energy of a rotational state having quantum number J is $E = BJ(J+1)$, where B/k is large compared to the temperatures studied here and has the value of 86 K for H_2, 64 K for HD, and 43 K for D_2. Thus only the $J=0$ and $J=1$ states were occupied for the experiments reported here.

Since the $J=0$ solid hydrogens (p-H_2, HD, and o-D_2) have all their rotational degrees of freedom frozen out, they should all have similar properties characterized by their respectively similar Debye temperatures. The $J=1$ solid hydrogens (o-H_2 and p-D_2) are different in that they possess the three additional degrees of freedom due to the rotational substates $m_J = \pm 1, 0$. In the nearly pure $J=0$ solids containing less than a few percent of $J=1$ impurities (for example the p-H_2 and HD samples used in the thermal conductivity measurements discussed here) the degeneracy of the $m_J = \pm 1, 0$ states is lifted by interactions such as the crystalline field and the electric quadrupole-quadrupole (EQQ) interaction. The strength of the interaction will be taken to be the same for both o-H_2 and p-D_2 impurities since both have about the same electric quadrupole moment. The resulting splittings of the m_J substates are of the order of kT and thus would be expected to effect the thermal properties of the solid.

A detailed calculation of the thermal conductivity of the solid hydrogens must include a complete account of the possible phonon scattering processes. Such a calculation is beyond the scope of this paper which is primarily concerned with the contribution to the thermal conductivity of the $J=1$ impurities in an otherwise $J=0$ hydrogen solid. Thus a detailed account of the scattering processes which are independent of J will not be given. Instead only those processes which are sufficient to explain the data will be considered.

It will be shown that umklapp scattering is unimportant in the data reported here. The data have been adequately explained by considering in addition to the phonon scattering due to the $J=1$ impurities the following processes: (i) boundary scattering which is characterized by a constant phonon lifetime, L/v, where v is the sound velocity and L is some length characteristic of the particular sample; (ii) normal three-phonon processes about which there is no previous experimental knowledge in the hydrogens; and (iii) isotopic impurity scattering which is proportional to fourth power of the phonon frequency.

B. Phonon Scattering by $J=1$ Impurities

The only existing calculation of the effect of $J=1$ impurities on the thermal conductivity of the $J=0$ solid hydrogens was made by Ebner and Sung.[2] They calculated the effect of o-H_2 impurities on the thermal conductivity of p-H_2. The calculation assumes that the only additional scattering mechanism obtained by replacing a p-H_2 molecule with an o-H_2 molecule is to allow a two-phonon Raman scattering by the rotational substates of the $J=1$ molecules.

At low temperatures the energy splittings of the $J=1$ substates are of the order kT. Consequently, a direct absorption or emission of a single phonon could occur and possibly limit the thermal conductivity. Prompted by the anomalously large $J=1$ scattering at the lowest temperatures, an estimate of the effect of the one-phonon process on the thermal conductivity was made using essentially the same assumptions as were made by Ebner and Sung. The calculation assumed that the coupling between the rotational substates and the lattice resulted from the dependence of the anisotropic valence and van der Waals interactions[11] on the intermolecular separation. By expanding the interaction in powers of the displacement of the molecules from their equilibrium positions and then replacing the displacements by the corresponding phonon operators, an explicit expression for the phonon coupling was obtained.[12] The term linear in the phonon operators thus corresponds to a one-phonon process and the quadratic term to the two-phonon process which was considered by Ebner and Sung.

Evaluation of the matrix elements that result from a calculation of the transition probability for the emission or absorption of a phonon requires a knowledge of the interactions which lift the degeneracy of the rotational substates. The measurements were done at low $J=1$ concentrations, thus the degeneracy of the rotational substates was lifted by the crystalline field created by the surrounding $J=0$ molecules and by pairwise $J=1$ interactions (triples or higher clusters are unlikely). The electric quadrupole-quadrupole interaction is usually taken to be the dominant pair interaction. The EQQ interaction produces a degenerate ground state which is in part lifted by the crystalline field.[13] The combined interactions thus produce a low-lying energy level having a splitting comparable to the crystalline field levels of an isolated molecule. Since all the rotational operators have matrix elements of the order unity and since only the low-lying rotational levels would be populated at the very low temperatures where the one-phonon process might be important, an evaluation of the transition probability assuming only a crystal-field splitting of the rotational substates would seem reasonable. The value of the splitting found from a fit to the experimental data should then represent some mean splitting from the ground state, the crystalline field, or a combination of these or other interactions.

The transition probability for the one-phonon process was related to the thermal conductivity through assumptions analogous to those made in the single-mode approximation for the two-phonon process.[14] Evaluation of the equivalent single-mode relaxation time for the one-phonon case differed from the two-phonon case primarily in that the phonon number for the second phonon was replaced by the number of $J=1$ molecules in a given initial and final rotational substate.

Evaluation of the relaxation time for the one-phonon process was done assuming $kT \gg A$, where A is the energy splitting of the rotational substates. In addition, an isotropic average was taken over the phonon orientations. The expression obtained for the inverse relaxation time was

$$\tau_1^{-1} = \left[(8Af^2\omega c)/(25\,kTmv^2)\right]\delta(\hbar\omega - A)\,, \qquad (1)$$

where ω is the phonon frequency; c is the $J=1$ concentration; v is the velocity of sound; m is the molecular mass ($\simeq 3$ amu); and $f = -(8\pi)^{1/2}(g'a_0 + 3g)$. The value of the intermolecular separation a_0 was taken to be 3.67 Å and the function g (related to the valence and van der Waals interaction) is given by

$$g = \epsilon_1 e^{-\eta(r-a_0)/a_0} - \epsilon_2 (a_0/r)^6\,, \qquad (2)$$

where r is the intermolecular separation between the interacting molecules (assumed only nearest neighbors). An estimate of the values of ϵ_1 and ϵ_2 can be obtained from the renormalized values for an o-H_2 molecule in otherwise p-H_2 given in Refs. 2 and 11, i.e., $\epsilon_1 = 4.00 \times 10^{-16}$ erg, $\epsilon_2 = 1.32 \times 10^{-16}$ erg, and $\eta = 13$. The values of ϵ_1 and ϵ_2 for o-H_2 and p-D_2 molecules in HD will be slightly different. However, the difference will likely be less than the uncertainty in the above values and thus no attempt has been made to refine the values above.

After taking an isotropic average, the value obtained from Ref. 2 for the inverse relaxation time of the two-phonon process is

$$\tau_2^{-1} = \left(\frac{6\epsilon_1\eta^2}{35mv^2}\right)^2 \frac{k\Theta_D c}{3\pi\hbar} \times \left\{\frac{2x^4T^4}{\Theta_D^4} + 0.138\,c\left[\frac{xT}{\Theta_D} + \frac{3x^2T^2}{\Theta_D^2}\right]\right\}, \qquad (3)$$

where $x = \hbar\omega/kT$ and the other symbols are as defined above. The term in the square brackets corresponds to inelastic phonon scattering and the x^4 term corresponds to elastic scattering.

C. Relationship between Thermal Conductivity and Phonon Relaxation Times

The frequency-dependent relaxation times given above must now be related to the thermal conductivity. A theory relating the relaxation times and the conductivity has been developed by Callaway.[15] He makes the usual assumptions that there is no dispersion in the lattice vibration spectrum, the crystal is elastically isotropic, and that the longitudinal and transverse phonon modes are indistinguishable. These assumptions are necessitated by a lack of detailed information about the crystal and have been adopted here.

Since normal processes cannot by themselves limit the thermal conductivity, any theory relating the thermal conductivity to the phonon relaxation times must distinguish between normal and other processes. The theory of Callaway reflects this distinction and depends on the normal process relaxation time τ_N in a complicated way. Since at present there is no *a priori* knowledge of the normal process scattering in the solid hydrogens, one is forced to investigate the limiting cases. The two natural limits are $\tau_N \to \infty$ and $\tau_N \to 0$. When $\tau_N \to \infty$ Callaway's expression for the thermal conductivity reduces to

$$\kappa = \frac{k}{2\pi^2 v}\left(\frac{kT}{\hbar}\right)^3 \int_0^{\Theta_D/T} \tau(x) J(x)\, dx \ , \tag{4}$$

where $\tau^{-1}(x)$ is the sum of the inverse relaxation times for the appropriate processes or $\tau^{-1} = \tau_1^{-1} + \tau_2^{-1} + \tau_B^{-1} + \tau_I^{-1} + \tau_U^{-1}$, where the subscripts on the inverse relaxation times τ^{-1} refer, respectively, to a first-order process, a second-order process, boundary scattering, impurity scattering, and umklapp scattering. The function $J(x)$ is given by

$$J(x) = x^4 e^x/(e^x - 1)^2 \ . \tag{5}$$

At low temperatures $\Theta_D/T \to \infty$ and the limits on the integral can adequately be taken from zero to infinity. It is noted that this is the limit Ebner and Sung used in their calculation of the thermal conductivity of p-H_2. In the limit $\tau_N \to 0$ the expression for the thermal conductivity becomes

$$\kappa = \frac{k}{2\pi^2 v}\left(\frac{kT}{\hbar}\right)^3 \left(\int_0^{\Theta_D/T} J(x)\, dx\right)^2 \Big/ \left(\int_0^{\Theta_D/T} \tau^{-1}(x) J(x)\, dx\right). \tag{6}$$

This limit corresponds to taking a harmonic average of the inverse relaxation times over the phonon distribution[16] and has the consequence that it is valid to add thermal resistances (inverse conductivities) due to the various scattering processes.

The contribution of the one-phonon process in the two limiting cases is quite different. When Eq. (4) is used to calculate the thermal conductivity, the one-phonon process given by Eq. (1) contributes only for the frequency $\omega = A/\hbar$ which is an insignificant effect. Even if the rotational energy levels were broadened about A such that the phonons in this band were ineffective in transporting energy, the total reduction in the number of phonons would be small. Thus one must conclude that in the limit $\tau_N \to \infty$ the one-phonon process does not limit the thermal conductivity.

In the limit $\tau_N \to 0$ the harmonic average over the δ function in Eq. (1) has a finite value. Thus in this limit the direct process does contribute to the thermal conductivity. Physically this results from the fact that when $\tau_N \to 0$ a phonon loses its frequency identity. A finite fraction of the life of a group of phonons will be spent in a frequency mode which is effectively scattered by the rotational substates.

Of the scattering processes considered here, only the one-phonon process accompanied by very rapid normal phonon scattering can account for the very rapid increase in thermal resistivity with decreasing temperature observed from the data. Further analysis of the data indicates that at high temperatures where isotopic scattering is important, the temperature dependence of the data is best fit using the limit $\tau_N \to 0$ in Eq. (6). Also the value obtained for the concentration of isotopic impurities is in reasonable agreement with the measured values. Considering the success of Eq. (6) and the failure of Eq. (4) to account for the isotopic scattering as well as the low-temperature data, the limit $\tau_N \to 0$ and Eq. (6) will be taken as the appropriate limit.

The values of the thermal resistance for the various processes have been calculated using Eq. (6) for later comparison with the data. The contribution to the thermal resistance calculated for the direct process was

$$\kappa_1^{-1} = 9\hbar^2 f^2 A^4 c/\pi^6 k^8 m v T^7 \ . \tag{7}$$

It is noted that when the high-temperature approximation for the populations of the rotational substates is valid ($A \ll kT$), the thermal resistance due to the one-phonon process is increasing as T^{-7} as the temperature is lowered. Thus this contribution to the thermal resistivity increases more rapidly than T^{-3} which is in contrast to all other processes considered. Examination of the complete expression for the thermal resistance due to the one-phonon process shows that the resistivity reaches a maximum when the peak in the phonon distribution corresponds to A or when $A \simeq kT$. The resistivity then decreases below this temperature.

Using Eqs. (3) and (6) the thermal resistance due to the Raman scattering by the rotational substates was found to be

$$\kappa_2^{-1} = \left(\frac{\epsilon_1^2 \eta^4 \hbar^2 c}{m^2 v^3 k^3}\right) [5.26\times 10^{-6}\, T + 1.57\times 10^{-3} c\,(T^{-2} + 0.158^{-1})] \ , \tag{8}$$

where $\Theta_D = 112$ K has been combined with the numerical values in the square brackets. The first term in brackets is due to elastic scattering and the second due to inelastic scattering.

The thermal resistance due to isotopic scattering can be found in Ref. 16 (p. 310) and is

$$\kappa_I^{-1} = 20\pi^3 (6\pi)^{1/3} v^2 \hbar^3 c_i\, T/a_0 k^4 \Theta_D^4 \ , \tag{9}$$

where c_i is the sum of the H_2 and D_2 impurity concentrations.

Boundary scattering is characterized by a frequency-independent phonon lifetime or free path L. The thermal resistance is then given by

$$\kappa_B^{-1} = (15 v^2 \hbar^3)/(2\pi^2 k^4 L T^3) \ . \tag{10}$$

Boundary scattering can show some temperature dependence depending on the degree of specular reflection of the phonons at the boundaries.[16] However, recourse to such a dependence was not needed to adequately explain the ($J = 1$)-independent scattering. Since only the ($J = 1$)-dependent scattering is of particular interest here, no further

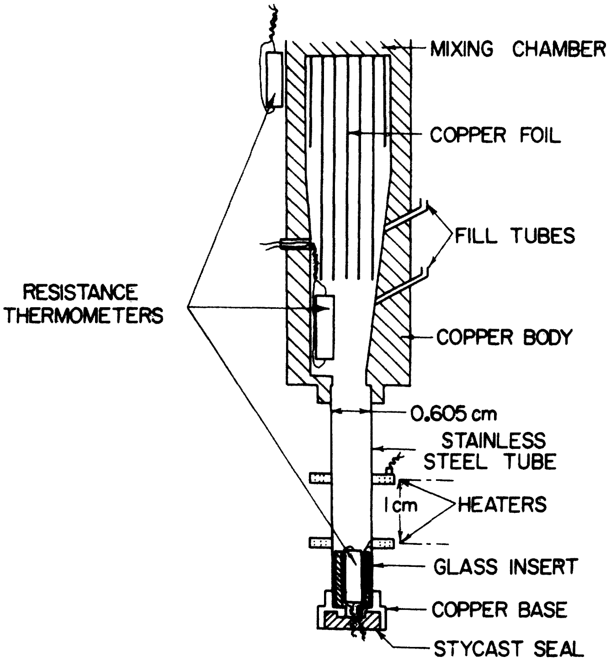

FIG. 1. Thermal-conductivity sample cell.

consideration of the degree of specular reflection will be made.

III. EXPERIMENTAL DATA

A. Measurement Technique

The solid HD thermal conductivities reported here were measured using the one-thermometer–two-heater technique. (See Ref. 1 for a description of this technique.) This method has the advantage that small temperature gradients across the sample can be measured accurately and that the heat flux into the sample from $J=1$ to $J=0$ conversion (or other means) does not effect the measurement so long as the temperature differential across the sample is small compared to the temperature.

The thermal conductivity sample cell is shown in Fig. 1. While the cell was filled with He^4, the two 220-Ω Speer resistance thermometers inside the cell were calibrated against the 220-Ω Speer resistor mounted on the outside of the mixing chamber of the dilution refrigerator. The resistor on the mixing chamber had been calibrated from the NMR susceptibility of platinum in earlier experiments. The calibration has been stable to within ± 5% over a period of three years.[5] The NMR calibration was shifted to zero magnetic field by repeating the last set of thermal conductivity measurements at the NMR field. Under the assumption that the thermal conductivity is independent of magnetic field, corrected temperatures were found with the largest correction being 2%.

The two matched 10 000-Ω heaters shown in Fig. 1 were made from 390 cm of Evanohm wire which was loosely coiled in the donut-shaped recess of the sample tube (height and outside diameter of the recess were 0.8 mm and 1.24 cm, respectively). This construction was chosen to provide a large HD to wire surface area and to remove from the main column of HD any local heating of the HD due to poor wire to HD contact. The spiral of copper foil at the top of the cell was used to make thermal contact to the solid HD. A description of the thermal conductivity cell including descriptions of the heaters, thermometers, and the method of making thermal contact is given in Ref. 17 where a preliminary account of these data was given.

The thermal conductivity of the empty cell was also measured using the one-thermometer–two-heater technique. To within 5% the empty-cell conductivity data could be fit by the expression

$$\kappa_c = (9.74T + 20.6T^3)\ \mu\text{W/K}\ . \tag{11}$$

The thermal conductivities measured when the cell was filled with HD were assumed to result from a parallel conduction of the sample cell walls and the column of HD. The HD conduction was obtained by subtracting from the measured conduction the cell conduction given in Eq. (11). In all cases the cell conduction was less than 8% of the measured conduction and thus did not introduce any appreciable uncertainty into the values of the HD thermal conductivities.

The thermometer in the bottom of the cell was used in conjunction with the one in the top of the cell to measure the temperature differential developed across the sample cell due to the residual heat flux into the sample. The magnitude of the heat flux was found by applying a known power Q to the bottom heater and measuring the resulting temperature differential $\Delta T'$, which was produced. Under the assumption that the heat flux into the sample was uniform over its length, the total heat flux q into the region of the sample between the two thermometers can be found from

$$q = \frac{Q\Delta T}{\Delta T' - \Delta T}\ . \tag{12}$$

In the empty cell experiment q was found to be less than 0.01 μW which corresponds to an upper limit on the residual heat flux into the cell. This limit was obtained from data taken at temperatures less than 0.2 K, since at higher temperatures the temperature differential produced by 0.01 μW would be far too small to measure.

B. Determination of $J=1$ Conversion Rate

The heat produced by $J=1$ to $J=0$ conversion was measured over a period of 400 h in a preliminary

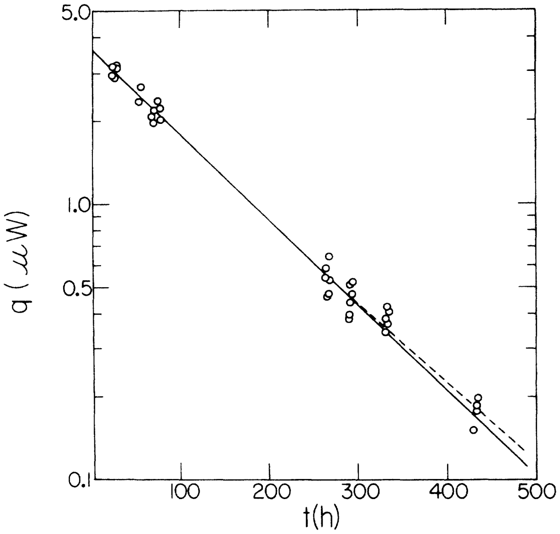

FIG. 2. Heat generated from $J=1$ to $J=0$ conversion of o-H_2 and p-D_2 impurities in solid HD vs the time that the HD had been solidified. The solid line is an exponential fit for $c_4=0$. The dashed curve is the best fit using the measured value of c_2 and $c4$.

experiment where accurate thermal conductivities were not obtained due to an open circuit in the top heater. A plot of the logarithm of q as a function of time obtained from this experiment is given in Fig. 2. During the time intervals indicated by the large time gaps in the data, the sample was kept at 4.2 K but otherwise the data were taken over the entire temperature range 4.2–0.2 K. However, only the data for temperatures less than 0.4 K are plotted since the temperature differential developed from the heat of conversion became too small to measure at higher temperatures. If one were to believe the results at these higher temperatures, they would indicate that the heat of conversion increased rapidly as the temperature was raised above 0.4 K. This apparent temperature dependence is the reason for most of the scatter in the data at a given time.

The conversion rate of the $J=1$ impurities in HD has been measured previously[18,19] and found to be in good agreement with the calculated rate.[20] From the previous experimental and theoretical work, it was inferred that the rate constant was independent of temperature and $J=1$ concentration for low $J=1$ concentrations. If the rate constant was constant or independent of concentration, then the o-H_2 and p-D_2 concentrations should decrease exponentially as should their conversion heat. It is seen in Fig. 2 that within experimental error the total conversion heat did decrease exponentially indicating a constant rate constant. The fact that the conversion heat decreased exponentially, apparently independent of thermal history, would also tend to support a temperature-independent conversion rate. The time constant obtained from Fig. 2 for the conversion rate was 141 ± 11 h. This time constant corresponds to the conversion rate of o-H_2 since in the experiments reported here the p-D_2 concentration was sufficiently low (see Sec. III C) that nearly all the conversion heat resulted from ortho-to-para conversion of hydrogen. The value of 141 ± 11 h obtained for the time constant agrees quite favorably with the value of 147 ± 11 h found in Ref. 19.

C. Impurity Concentrations

The concentrations of the H_2 and D_2 impurities in the HD were determined by NMR and mass spectroscopy. NMR provides a relatively easy way to reliably determine the constituents in HD samples even for very small concentrations of the various spin species. Mass spectroscopy, on the other hand, is susceptible to errors due to the reaction

$$\mathrm{HD}+\mathrm{HD}\rightarrow \mathrm{H}_2+\mathrm{D}_2 \qquad (13)$$

taking place in the ionized gas in the spectrometer. A mass spectroscopic determination of small concentrations of H_2 and D_2 in HD is thus difficult.

The NMR determinations of the H_2 and D_2 concentrations were made by measuring the proton and deuteron spin-lattice relaxation time, T_{1P} and T_{1D}, respectively, before and after successive dilutions of the HD by a known amount of normal H_2 and D_2. It has been shown that at low temperatures where diffusion is negligible T_{1P} and T_{1D} in a solid HD sample are given by [18,19]

$$T_{1P}=\frac{\frac{3}{8}N_3+\phi N_2}{\phi N_2}\,\tau_P\ , \qquad (14)$$

$$T_{1D}=\frac{N_3+\frac{1}{2}(5-3\theta)N_4}{\theta N_4}\,\tau_D\ , \qquad (15)$$

where N_2, N_3, and N_4 are, respectively, the number of H_2, HD, and D_2 molecules in the sample, ϕ and θ are the $J=1$ fractions of the H_2 and D_2, respectively, and τ_P and τ_D are the inherent spin lattice relaxation times of the $J=1$ H_2 and D_2 molecules. The inherent relaxation of the o-H_2 and p-D_2 molecules is due to the molecular reorientations of these molecules, and consequently the relaxation time can be expressed as a product of a function of the correlation times for the molecular reorientations and a matrix element giving the effectiveness of the reorientations in producing relaxation. Since the o-H_2 and p-D_2 quadrupole moments are nearly equal, the correlation times of the two molecules will be nearly equal and depend only on the total $J=1$ concentration. The matrix elements for o-H_2 and p-D_2 differ but are independent of concentration. The ratio of τ_P and τ_D is thus a constant independent of $J=1$ concentration.

The T_1 measurements were made at 3 MHz by condensing the HD sample into the bottom of a glass tube inserted into a helium Dewar. Since the HD gas used in the experiment was stored at room temperature for over three months, it is reasonable to assume that the H_2 and D_2 in the sample were present in the normal rotational state. Thus the values of ϕ and θ were taken to be $\frac{3}{4}$ and $\frac{1}{3}$, respectively.

Using the fact that τ_P/τ_D is a constant, and using Eqs. (14) and (15), the expression connecting the relaxation times in the diluted and undiluted samples was found to be

$$\frac{T_{1D}}{T_{1P}}\,\frac{T'_{1P}}{T'_{1D}}=\frac{N_3+2N_4}{N_3+2N'_4}\,\frac{N'_4}{N_4}\ , \tag{16}$$

where T'_{1D}, T'_{1P}, and N'_4 are the respective quantities in the sample after it had been diluted with a given quantity of normal D_2. The expression connecting the relaxation times in the doubly diluted sample was similarly found to be

$$\frac{T''_{1P}}{T'_{1P}}\,\frac{T'_{1D}}{T''_{1D}}=\frac{N_3+2N''_2}{N_3+2N_2}\,\frac{N_2}{N''_2}\ , \tag{17}$$

where T''_{1D}, T''_{1P}, and N''_2 are the respective quantities in the sample after it had been diluted by both the normal D_2 and H_2. Equations (16) and (17) were solved simultaneously for $c_2=N_2/N$ and $c_4=N_4/N$, where c_2 and c_4 are the respective H_2 and D_2 concentrations in the original HD sample and $N=N_4+N_3+N_2$. The resulting fourth-order equation in the concentrations was solved numerically (although the fourth-order terms in c could have been dropped) and yielded $c_4=0.63\pm0.07\%$ and $c_2=1.7\pm0.4\%$ where the errors were obtained from the absolute uncertainty in the T_1 measurements.

Two mass spectroscopic analyses were performed on the HD. The first was done using a MS-90 Veeco leak detector set up to detect both masses three and four. A calibration of the relative sensitivity versus pressure was done using D_2 and HD. From this analysis the D_2 concentration was found to be $c_4=0.8\pm0.2\%$ which was in agreement with the NMR determination. Assuming both measurements were reliable, the agreement between the two indicates that the D_2 in the HD was in its normal rotational state.

A commercial mass spectroscopic analysis of the HD gas was also obtained. The results of this determination were $c_2=(3.54\pm0.04)\%$ and $c_4=(2.39\pm0.06)\%$. These results are significantly higher than the other determinations. It is believed that the reaction in Eq. (13) was responsible for this discrepancy in which case the results for the H_2 and D_2 concentrations found from this determination should differ from the previous values by the same percentage. Subtracting the NMR determination from the commercial mass spectroscopic values yields 1.8% for the H_2 concentration and 1.76% for the D_2 concentration which are the same to within experimental accuracy. In view of the consistancy of the three determinations under the assumption of dissociation in the commercial mass spectroscopic analysis, the H_2 and D_2 concentrations in the experiment have been taken to be the values determined from the NMR determination ($c_2=1.7\%$ and $c_4=0.63\%$). It should be pointed out that an error in the concentration determination only affects the absolute magnitude of the ($J=1$)-dependent one- and two-phonon scattering processes and not the significant qualitative agreement between the experiment and theory heretofore unobserved.

The $J=1$ concentration as a function of time is given by

$$c(J=1)=\phi c_2 e^{-t/D}+\theta c_4 e^{-\xi t/D}\ , \tag{18}$$

where c_2 and c_4 are the H_2 and D_2 concentrations given above; ϕ and θ were again taken to be $\frac{3}{4}$ and $\frac{1}{3}$, respectively; D is the time constant for the ortho-para conversion in H_2 which was found in Sec. III B to equal 141 h under the assumption $c_4=0$; and ξ is the ratio of the time constants for o-H_2 and p-D_2 conversion. The value of ξ was obtained from the ratio of the theoretical rate constants obtained from Ref. 20 and has the value of $\xi=0.54$. The heat generated in the sample from conversion of the $J=1$ molecules is given by

$$Q=(172\,kN/D)\left[\phi c_2 e^{-t/D}+\left(\tfrac{1}{2}\theta\xi c_4\right)e^{-\xi t/D}\right]\ , \tag{19}$$

where $172\,k$ is the energy spacing between the $J=1$ and $J=0$ rotational states of o-H_2 and k is the Boltzmann constant. An improved value for D can now be obtained by fitting Eq. (19) to the data in Fig. 2 and using the measured values of c_2 and c_4. This was done and the value found was $D=138\pm11$ h. The resulting fit is given by the dashed curve in Fig. 2. The previous result ($D=141$ h) was obtained assuming $c_4=0$.

D. Conductivity Data

Figure 3 shows the thermal-conductivity data taken at two different time intervals during the 271 h which the sample was frozen. During this period Eq. (18) shows that the $J=1$ concentration changed from 1.5% to 0.2%. The points on curve (a) in Fig. 3 were taken between 22 and 28 h after the sample was condensed with the mean time being 26 h. This time corresponds to a $J=1$ concentration of 1.2%. The points on curve (b) were taken between 260 and 271 h after the sample was condensed into the sample cell. The mean time was 264 h corresponding to a $J=1$ concentration of 0.25%.

Figure 3 shows that thermal conductivity did depend on the time the sample was frozen and consequently on the $J=1$ concentration. Under the assumption that the appropriate method of averaging over the phonon distribution is given by Eq. (6),

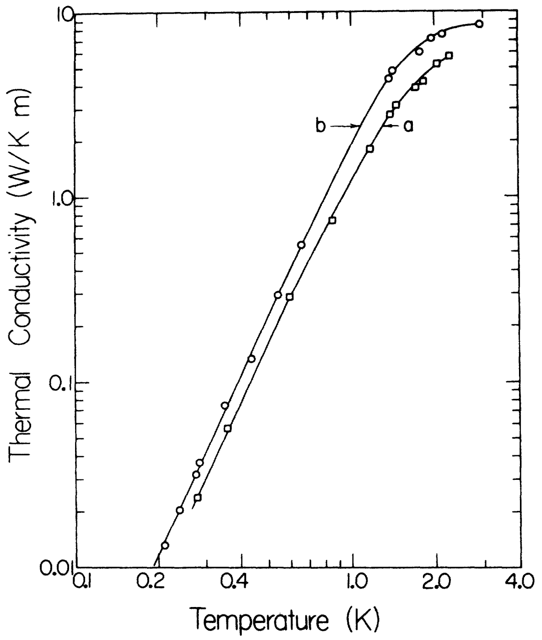

FIG. 3. Measured HD thermal conductivities taken during two different time intervals after solidification. The mean time for the points on curve (a) was 26 h whereas the mean time for the points on curve (b) was 264 h.

the concentration and temperature dependence of the $J=1$ phonon scattering can be obtained by subtracting from the thermal resistance (reciprocal conductivity) at a given time, the thermal resistance at infinite time corresponding to a zero $J=1$ concentration. The calculated thermal resistance is obtained by adding the thermal resistances in Eqs. (7)–(10) which yields an expression of the form

$$\kappa^{-1}=\alpha c T^{-7}+\beta c[\sigma T+c(T^{-2}+0.185\,T^{-1})]+\gamma T^{-3}+\delta T\,, \tag{20}$$

where $\sigma=3.34\times10^{-3}$ and α, β, γ and δ are constants which can be deduced from Eqs. (7)–(10). Subtracting the thermal resistances consequently yields the first two terms in Eq. (20).

No appreciable change in the thermal conductivity with time was observed by the time the points on curve (b) of Fig. 3 were taken. Thus for all practical purposes this curve can be considered the $c=0$ curve and subtracted from the other curves to obtain the $J=1$ dependence of the thermal resistance. Curve (e) of Fig. 4 was obtained by subtracting from the thermal resistances obtained from the points on curve (a) of Fig. 3 the thermal resistance obtained from the line through curve (b) of Fig. 3. Curve (f) was obtained by subtracting the resistances obtained from curve (b) from the points taken between 164 and 173 h after the sample was condensed. The mean time was 169 h and corresponds to a $J=1$ concentration of 0.47%.

Inspection of the first two terms in Eq. (20) shows that at the higher temperatures the first term in the square brackets, (σT), should start to become dominant. The dot-dash line proportional to T^{-2} drawn through the high-temperature data in curves (e) and (f) indicates that the resistivity differences at a given time or concentration are very nearly proportional to T^{-2} and not to T. Under the continued assumption that it is correct to add thermal resistivities, it must be concluded that the estimate of the elastic scattering of the $J=1$ impurities given in Ref. 2 must be much too large in comparison to the estimate of the inelastic scattering.

The ratio of the thermal resistivities at 1.5 K taken from the T^{-2} lines drawn through the high-temperature data in curves (e) and (f) is 6.5. The ratio of the squares of the average concentrations is 6.5. A comparison of these two ratios shows that at the higher temperatures the concentration dependence of the $J=1$ scattering is c^2. Consequently, the $(J=1)$-dependent thermal resistivity is described adequately between 3 and 1 K by a resistivity of the form $R=\beta c^2 T^{-2}$.

At temperatures below 0.5 K, the resistivity due

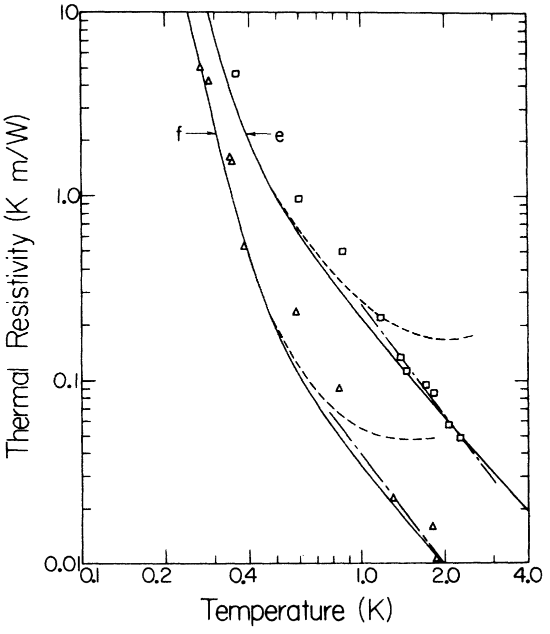

FIG. 4. The $(J=1)$-dependent thermal resistivity. The squares correspond to resistivities obtained by subtracting curve (b) of Fig. 2 from the points on curve (a). The triangles correspond to subtracting curve (b) from points taken during an interval having a mean time of 169 h. The solid lines were obtained from a least-squares fit to all the data assuming $\sigma=0$ in Eq. (21). The dashed line corresponds to a fit assuming $\sigma\neq0$. The dashed-dot line is a T^2 fit to the high-temperature resistivities.

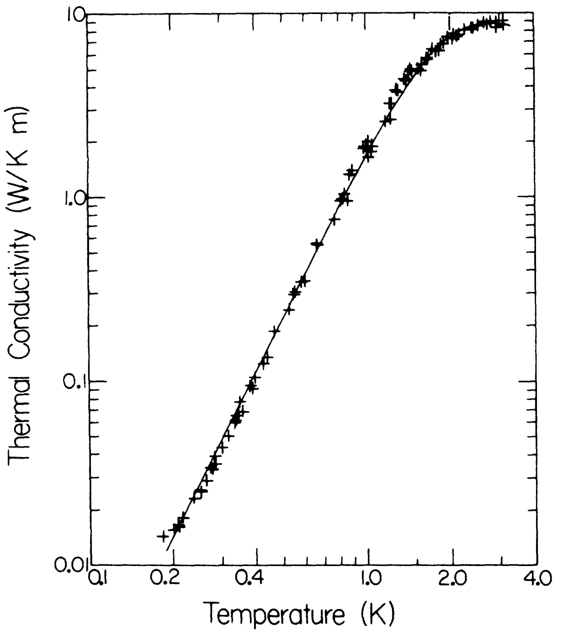

FIG. 5. The $(J=1)$-independent conductivity obtained by subtracting the $(J=1)$-dependent thermal resistivity given in Eq. (21) from the measured thermal resistivities. The width of the error bars represents the ± 5% uncertainty in the temperature. The solid line corresponds to the least-squares fit to all the data.

to the $J=1$ impurities is seen to increase with decreasing temperature more rapidly than T^{-2} or even T^{-3}, implying that the phonon scattering probability must be increasing as the temperature is decreased. Such a temperature dependence is in general not found in the two-phonon processes. The requirement that only the sum or difference of the two-phonon energies be equal to the change in energy of the rotational substates does not severely limit the band of phonon frequencies that can be scattered. However, in the one-phonon process, the resonant requirement produces a scattering which is most effective for the band of phonons surrounding the resonant frequency. Consequently, as the peak in the phonon distribution approaches the resonant frequency a greater fraction of the phonons can be scattered and the thermal resistance increases as the temperature is decreased. The fact that the thermal resistance resulting from the one-phonon process was expected to increase with decreasing temperature motivated the calculation of the resulting thermal resistivity appearing in Eq. (7). To within the accuracy of the experimental data, the rapidly increasing resistivity appearing below 0.5 K is fitted by Eq. (7). However, the tentative assignment of this scattering to a one-phonon process should not be taken too seriously. The small number of experimental points taken where this process is significant provides a very limited test of the theoretical predictions and even the theory is derived on the unjustified assumption that Eq. (6) is the appropriate average to take over the phonon distribution. In addition, no explicit account has been taken of the other possibilities such as the validity of the high-temperature approximation used in Ref. 2 or of the possibility of thermal transport of rotational or nuclear-spin energy.

The results of a least-squares fit to all the data are given in the following paragraphs where further justifications will be given for the choice of the phonon average given in Eq. (6) over that given in Eq. (4). The lines drawn through the points in curves (e) and (f) of Fig. 4 were obtained from a resistivity of the form

$$R_1 = \alpha c T^{-7} + \beta c^2 (T^{-2} + 0.185\, T^{-1} + \sigma T/c)\,, \qquad (21)$$

where the values of α and β were obtained from the least-squares fit to all the data and c was taken to be the average $J=1$ concentration given earlier for curves (e) and (f). The dashed line corresponds to the value of σ obtained from Ref. 2 ($\sigma = 3.3\times10^{-3}$) and the solid curve corresponds to $\sigma = 0$. The overestimate of the value of σ given in Ref. 2 can again be seen from the two curves.

The results of a computer fit to Eq. (20) using all the data and the $J=1$ concentration given by Eq. (18) were $\alpha = 0.099$, $\beta = 1.32\times10^{3}$, $\gamma = 0.57$, and $\delta = 0.031$, where σ was taken to be zero and the units are ($\mathrm{m\,K}^{n}/\mathrm{W}$) with n taking the appropriate values for the four terms. Figure 5 shows a plot of the $J=1$ concentration-independent thermal conductivity. The points were obtained by subtracting from the measured value of the thermal resistance the thermal resistance obtained from Eq. (21) using the values of α and β given above. The line drawn through the data was obtained using the third and fourth terms in Eq. (20) and the values of γ and δ given above.

Examination of Fig. 5 shows that the four-parameter fit of Eq. (20) accounts for the data fairly well and consequently other resistive mechanisms are probably not of significant importance. Because the umklapp process is often important at temperatures around the conductivity maximum and above, it requires further consideration. The magnitude of the umklapp resistivity should be about the same in both p-H_2 and HD since both are hydrogen solids having about the same Debye temperature. In the p-H_2 experiment the umklapp process was found to be significant in limiting the thermal conductivity near the conductivity peak. From a fit to the p-H_2 data,[21] the umklapp thermal resistivity was found to be $R_u = 8.3\times10^{4}\, T^{-3} \exp(-109/2\,T)$ m K/W. A comparison of this resistivity to the ones obtained from Fig. 3 shows that the umklapp resistivity is less than 2% of the total HD resistivity for all measured temperatures and thus can be neglected. The reason the umklapp scattering is less important in the HD data than the p-H_2 data is because of the reduction of the HD thermal conductivity near the conductivity maximum due to the higher concentration of isotopic impurities.

A value for the concentration of isotopic impurities can be obtained by equating the value of δ obtained from the data to the value calculated from Eq. (9). The value obtained was 1.52% and compares favorably with the 1.7% H_2 and the 0.63% D_2 known to be in the sample (see Sec. IIIC). The overestimate of the isotopic scattering given when the measured H_2 and D_2 concentrations are used in Eq. (6) would tend to indicate that the limit $\tau_N \to 0$ used to obtain Eq. (9) is not an ideal assumption. However, when the other extreme is tried, $\tau_N \to \infty$, the agreement is extremely poor. Thus of the two extremes, Eq. (6) is the most satisfactory. The discrepancy might also be due to other factors such as a cluster of impurities or quantum crystal effects.[22]

From the value of γ obtained from the data, one can deduce the temperature-independent mean free path which is generally taken to be the typical dimension of the crystallites in the sample. The value found for L was 64 μm. Since no $J=1$ concentration dependence of L was observed in the HD data, the apparent dependence of L on the $J=1$ concentration found in the p-H_2 data of Ref. 1 would seem to arise from the solidification process and not the ortho-para ratio in a given crystal.

One interesting feature of the data not accounted for in the theory is the small jump in the conductivity at about 1.5 K. This effect can be seen in Fig. 5 by noting that above 1.5 K the data are centered on the fitted line, however; below 1.5 K the data are centered above the fitted line. Although it is possible that this is due to experimental scatter, it is interesting to speculate (based on the regularity of the deviation) that it may originate from some degree of ordering in the sample. One possibility would be an isotopic phase segregation which could have occurred on solidification in which case a cooperative transition[23] could occur in the enriched $J=1$ domains at 1.5 K. Similar experimental results have been observed in solid helium[24] where phase separation occurs in the solid.

E. Contact Resistance

In this experiment and in the ones done prior to it,[4,5] measurements have been made of the thermal resistance resulting from making thermal contact to the hydrogen samples. Both hydrogen to copper and hydrogen to liquid-helium interfaces have been used. In all cases the results of these measurements have yielded a substantially higher thermal resistance than would be expected from the Khalatnikov theory of boundary resistance.[6]

A spiral of copper foil was used to make thermal contact to the HD for the thermal-conductivity measurements. The results obtained for the contact resistance in this case were given in Ref. 17. After completion of the thermal-conductivity experiment, some of the HD was removed from the cell and replaced by liquid He^4 which was condensed into the cell under its own vapor pressure. A calculation of the temperature differential developed across the He^4 column demonstrates that it was negligibly small compared to the one across the HD. The temperature differential δT developed across the thermal contact resistance R_c and the bulk thermal resistance of the HD κ^{-1} from a power Q applied to the upper heater is the difference between the temperature measured on the top and bottom thermometers inside the sample cell. Neglecting the small conversion heat remaining after 300 h and the cell-wall conduction, the heat-flow equation is

$$\delta T = (Q/A)(R_c + l_2 \kappa^{-1}) , \tag{22}$$

where l_2 is the length of sample above the top heater. By switching the heater power to the lower heater, κ^{-1} was found as before from the change in temperature ΔT of the lower thermometer. Substitution of the expression for κ^{-1} into Eq. (22) yields

$$\delta T/\Delta T = l_2/l_1 + (Q/AT^3\Delta T)(R_c T^3) , \tag{23}$$

where l_1 is the separation of the two heaters. A plot of $\delta T/\Delta T$ vs $(Q/AT^3\Delta T)$ was found to yield a straight line for temperatures below 0.6 K. At higher temperatures the He^4 conductivity in the fill tubes became dominant. From the slope of the plot obtained from Eq. (23), the value of $R_c T^3$ was found to be 1.1×10^{-5} cm^2 K^4/μW and from the intercept, l_2/l_1 was found to be 0.05. Although this value of RT^3 is closer to the value expected for a pure boundary resistance than the previous values,[4,5] the resistivity above what would be expected is likely due to the fact that the sample is very porous at the top and consequently has a much poorer thermal conductivity. Two observations have been made which substantiate this interpretation. (i) The addition of He^3 to the liquid He^4 used for thermal contact substantially improves the thermal contact. Reasonable quantitative agreement for the improvement can be accounted for on the basis of the improved thermal conductivity of the liquid helium in the narrow channels of the porous hydrogen.[4] (ii) The small value of l_2/l_1 obtained above indicates that the height l_2 of the effective bulk HD is much less than the approximate 1 cm expected from the amount of HD gas emitted to the sample cell. Thus the conductivity through the upper portion of sample was possibly due to conduction through the liquid helium.

It is presently believed that the difficulty encountered with hydrogen to copper thermal contacts is due to fractures of the crystal around the copper and subsequent pulling away of the crystal from the copper upon cooling. Liquid helium eliminates this problem, however; the conduction through the porous region of the sample near the top limits the heat that can be removed from the sample. All the samples that have been studied have been grown under their own vapor pressures. Thus a possible solution to the contact problem is to pressurize the hydrogen gas prior to solidification so that when the sample is cooled the sample does not contract away from the copper contact.

IV. DISCUSSION

A. Significance of Coefficients α and β

The magnitudes of the coefficients α and β are related through their dependence on the anisotropic part of the valence and van der Waal's interactions for the coupling which gives rise to the phonon scattering. As mentioned earlier, the strength of these interactions is not accurately known. If the rotational matrix elements resulting from the calculation of the thermal conductivity could be evaluated, then the coefficients α and β would determine the magnitudes of the anisotropic valence and van der Waal's interactions.

In the case where the two-phonon process is dominant, scattering takes place between all nine of the rotational pair substates created by the EQQ interaction. The matrix elements for this case can be evaluated fairly accurately since the magnitude of the EQQ interaction is known quite well. However, at lower temperatures where the one-phonon process is dominant, only the low-lying rotational substates are important because only these states are accessible to the low-energy thermal phonons. It is the origin of these low-lying states which is uncertain making an unambiguous evaluation of the valence and van der Waal's interactions impossible.

One possibility is that the one-phonon process is taking place exclusively between the near continuum of EQQ levels formed in a nearly pure $J=0$ ortho-para alloy. A numerical evaluation of the effect of these levels on the thermal conductivity showed that, in the temperature range 4–0.2 K, these states gave rise to a maximum in the thermal resistivity around 0.6 K. Further, the magnitude of the resistivity was less than that expected from the presence of only a crystalline field splitting of the rotational substates. Consequently, a one-phonon process taking place between the pure EQQ levels does not account for the rapid increase in the $(J=1)$-dependent thermal resistivity below 0.5 K. Scattering between the EQQ states could account, however, for the departure from the curves fitted through the resistivity differences in Fig. 4. It is noted that the experimental points lie above the fitted curve and show a maximum departure just where the EQQ levels would be expected to give a maximum resistance.

The numerical calculation of the effect of the EQQ interaction was carried out using the EQQ pair wave functions and summing over the first 3044 possible pair separations weighted by their probability. The probability of a given pair separation was taken to be the probability of having two $J=1$ molecules with the given separation times the probability that there were no other $J=1$ molecules inside two spheres (with radii equal to the separation of the two $J=1$ molecules) centered on the two given $J=1$ molecules.

Assuming then that the one-phonon process is solely due to a crystalline field splitting of the rotational substates, an accurate determination of the value of A can be obtained by comparing the magnitude of the coefficients α and β. The ratio of α to β is given by the ratio of Eq. (7) to Eq. (8) as

$$\frac{\alpha}{\beta}=\frac{5.96\,mv^2f^2A^4}{\epsilon_1^2\eta^4k^5} \quad . \tag{24}$$

Thus the value of A determined from Eq. (24) depends experimentally only on the fourth root of the ratio of α to β. In addition, the principal dependence of A on the magnitude of valence and van der Waal's interaction is through the square root of the value of η since $f/\epsilon_1\eta$ is of order unity. Solving for the value of A from Eq. (24) using the values given earlier for the various parameters yields $A/k=24$ mK. [Note that this value of A justifies the use of the high-temperature approximations used to obtain Eq. (1).] In the case of p-H_2 the most recent work places the value of A/k between 0.1 and 0.008 K.[25,26] A recent NMR determination of A/k in HD led to the value of $A/k=0.015$ K.[27] Comparing these results it can be seen that the value of A/k determined from the thermal-conductivity data is in reasonable agreement with the other determination.

The value of $\epsilon_1\eta^2$ determined from β and Eq. (8) was 1.53×10^{-20} J. This is 2.3 times larger than the value deduced from the parameters following Eq. (2). The factor of 2.3 is reasonable considering that the estimates given by various authors (Refs. 2, 11–13) differ by a larger factor. Also, a value of $\epsilon_1\eta^2$ has not been calculated explicitly for HD, the calculation of the value for p-H_2 includes a factor of 2.8 due to zero-point renormalization,[2] and the value of $\epsilon_1\eta^2$ needed to be increased by a larger factor for the theory of Ref. 2 to fit the p-H_2 thermal-conductivity data in Ref. 1.

B. Summary

The HD thermal-conductivity measurements reported here have shown a dependence on the $J = 1$ concentration qualitatively similar to that found in the p-H_2 measurements.[1] However, the fact that the $J = 1$ to $J = 0$ ratio was changed by conversion while the sample remained frozen allowed a separation of those phonon scattering mechanisms which depend on the $J = 1$ to $J = 0$ ratio and those which depend on the impurity concentration. The HD data showed that the anomalous T^3 dependence of the p-H_2 data on the o-H_2 concentration is not due to the $J = 1$ to $J = 0$ ratio in the sample but rather a property which is frozen in the crystal upon solidification. In the case of HD, consistency is found in attributing the anomalously large T^3 dependence of the thermal-conductivity data to a polycrystalline sample having voids or channels into which liquid helium can penetrate and carry heat. As these measurements are limited to the region below the thermal-conductivity maximum[28] and the sample was polycrystalline, no anisotropic effects should be expected.

The dependence of the HD thermal conductivity on the $J = 1$ to $J = 0$ ratio at high temperatures was found to be consistent with the theory of Ebner and Sung[2] with the exception that the elastic scattering term had to be dropped. At low temperatures a ($J = 1$)-dependent phonon scattering was found that increased rapidly with decreasing temperature down to the lowest temperature reported (~ 0.2 K). It has been found consistent to attribute this scattering to a direct absorption or emission of one phonon by the rotational substate of the $J = 1$ molecules. For a one-phonon process to effectively limit the thermal conductivity, the normal three-phonon processes must be very rapid. Substantiating evidence for the presence of rapid normal processes was obtained from the observed isotopic scattering. If the normal processes were not rapid, then the known isotopic impurities would not be sufficient to account for the magnitude or temperature dependence of the data. In conclusion, it is noted that theoretical fit to the data yielded values of the effective crystalline field splitting and interaction strengths which were within the limits of the presently accepted values.

[†] Work supported in part by a grant from the National Science Foundation No. GH-33011X.

[1] R. G. Bohn and C. F. Mate, Phys. Rev. B **2**, 2121 (1970).

[2] C. Ebner and C. C. Sung, Phys. Rev. B **2**, 2115 (1970).

[3] L. I. Amstutz, J. R. Thompson, and H. Meter, Phys. Rev. Lett. **21**, 1175 (1968).

[4] J. H. Constable and J. R. Gaines, Bull. Am. Phys. Soc. **16**, 88 (1971).

[5] J. H. Constable and J. R. Gaines, *Temperature, its Measurement and Control in Science and Industry* (Instrument Society of America, Pittsburgh, 1972), Vol. IV.

[6] I. M. Khalatnikov, Zh. Eksp. Teor. Fiz. **22**, 687 (1952).

[7] R. W. Hill and O. B. Lounasmaa, Philos. Mag. **4**, 785 (1959).

[8] R. J. Roberts and J. G. Daunt, J. Low Temp. Phys. **6**, 97 (1972).

[9] G. Ahlers, J. Chem. Phys. **41**, 86 (1964).

[10] M. Nielsen, Phys. Rev. B **7**, 1626 (1973).

[11] T. Nakamura, Prog. Theor. Phys. **14**, 135 (1955).

[12] J. Van Kranendonk and V. F. Sears, Contemp. Phys. **44**, 313 (1966).

[13] A. B. Harris, Phys. Rev. B **1**, 1881 (1970).

[14] P. Carruthers, Rev. Mod. Phys. **33**, 92 (1961).

[15] J. Callaway, Phys. Rev. **113**, 1046 (1959).

[16] J. M. Ziman, *Electrons and Phonons* (Clarendon, Oxford, 1960).

[17] J. H. Constable and J. R. Gaines, *Proceedings of the Thirteenth International Conference on Low Temperature Physics*, Boulder, Colo., edited by R. H. Kropshot and K. D. Timmerhaus (University of Colorado Press, Boulder, Colo., 1973).

[18] W. N. Hardy and J. R. Gaines, Phys. Rev. Lett. **17**, 1278 (1966).

[19] R. S. Rubins, A. Feldman and A. Honig, Phys. Rev. **169**, 299 (1968).

[20] K. Urano and K. Motizuki, Solid State Commun. **5**, 691 (1967).

[21] R. G. Bohn, thesis (The Ohio State University, 1969)(unpublished).

[22] R. D. Nelson and W. M. Hartmann, Phys. Rev. Lett. **28**, 1261 (1972).

[23] J. Felsteiner, Phys. Rev. Lett. **15**, 1025 (1965).

[24] A. E. Burgess and M. J. Crooks, Phys. Lett. **39A**, 183 (1972).

[25] W. N. Hardy and J. R. Gaines, Phys. Rev. Lett. **19**, 1417 (1967).

[26] J. H. Constable and J. R. Gaines, Solid State Commun. **9**, 155 (1971).

[27] J. H. Constable and J. R. Gaines (unpublished).

[28] E. M. Hogan and R. A. Guyer, Solid State Commun. **5**, 909 (1967).